2. Methods

2.1 Calculation with a modified MIRD-type phantom

An adult MIRD-5 type phantom [8] designed by Cristy was used to calculate enamel dose and organ doses against external photon exposure. A region for teeth was newly defined in the head of the phantom [9]. Figure 1 shows an overview of the MIRD type phantom and a cross section of the head at the level of newly added teeth area. The teeth were grouped into five parts to examine the distribution of the enamel dose in the mouth. Tooth enamels, however, were not specified in the teeth model. The elemental composition for the teeth region was based on the data for a whole tooth in ICRP Publication 23 [10]. Two kerma factors for a whole tooth and tooth enamel were prepared to calculate the enamel dose [9].

The Electron Gamma Shower Code Version 4 (EGS4) [11] in conjunction with user's code UCGEN [12] was used to calculate absorbed dose to organs and tissues. The data of photon cross section used in the radiation transport were taken from the library edited by Turbey *et al* [13]. Eight energies of incident photons were selected in the region between 30 keV and 2500 keV. Photon parallel beams were assumed to be incident on the phantom. Calculations were performed for 12 incident angles with 30 degrees interval to study the angular characteristics of the enamel dose and organ doses.

2.2 Experiment

Experiments were made with a realistic head phantom, which is made of tissue-equivalent plastic and contains human skull. The trunk of an Alderson RANDO phantom was connected to the head phantom to take radiations scattered by a human body into account. Teeth were inserted in the upper and lower jaws of the phantom. The phantom was exposed to gamma rays emitted from a ^{60}Co source in Anterior-Posterior (AP) and Posterior-Anterior (PA) geometries. After the irradiation, dental enamels were separated mechanically from other parts of the teeth and subjected to ESR measurements.

In addition to the tooth samples, thermoluminescence dosimeters (TLDs) were set in the head phantom to measure the absorbed dose to the teeth region. The TLD is made of a $CaSO_4$ crystal and has a diameter of 4mm. Two gamma ray sources of ^{60}Co and ^{137}Cs were used.

2.3 Calculation with a Voxel-type phantom

A generally called "Voxel (volume pixel)-type" phantom [14), 15)] was constructed from computed topography (CT) images of the physical phantom, which had been taken with 1mm interval. One CT image has 512x512 pixels (picture elements). Each pixel in the CT images was segmented into soft tissue area, bone area, teeth area and cavity area, according to its CT value and location. Tooth enamels, however, could not be distinguished from other parts of teeth.

Absorbed dose to the teeth region was calculated by using the EGS4 code in conjunction with user's code UCPIXEL [16]. Eight energies of incident photons were selected in the region between 30 keV and 2500 keV. The AP and PA geometries were considered for irradiations of photon parallel beam. The material of teeth region was defined as a whole tooth or $CaSO_4$ to verify results of the experiments. The enamel dose was derived with two kerma factors for a whole tooth and dental enamel as described in section 2.1.

3. Results and discussion

3.1 Doses calculated by using the modified MIRD-type phantom

Some of calculated enamel doses and organ doses are listed in Table 1 [9]. The values in the Angl (Avr.) geometry were obtained by averaging the doses all over horizontal incident angles. The data are given in the form of the ratio of the organ or tissue dose to the air kerma, in the unit of Gy/Gy. The results show significant dependence of enamel dose on energy and direction of incident photons.

Figure 2 depicts the calculated doses as a function of photon energy for the Angl (Avr.) geometry. The enamel dose indicates different behavior from other organ or tissue doses for low photon energies. Since tooth enamel contains elements with higher atomic numbers such as calcium and phosphorus more than soft tissue and bone tissue, the enamel dose increases due to energy absorption through photoelectric effect. On the other hand, the enamel dose is near to other organ doses in the energy region above 300 keV, where the Compton scattering process is dominant interaction with tissues.

Figure 3 shows the dependence of enamel dose and some organ doses on the incident direction of 1250keV photons. Since teeth are located at the front part in the head, the absorbed dose to enamel is smaller than dose to the colon in the PA geometry. On the contrary, the enamel dose is larger than the colon dose for the lateral irradiation geometries, because colon is well shielded by the human body tissues. The angular dependence of the enamel dose is similar to that of dose to the thyroid, which is located just below teeth.

3.2 ESR dosimetry and dose measurements with TLDs

Table 2 summarizes distributions of the enamel dose in the mouth obtained by the ESR dosimetry and the calculations for a ^{60}Co source. Since the relation between intensity of the ESR signal and enamel dose has not been determined yet, the ESR signal of teeth at the middle- and the back- part are given with relative values to those at the front part, which are normalized to 1.0. The values in the calculations are based on the result of 1250keV photons. The results of the ESR dosimetry agree with those of the calculation for the AP geometry. A steep gradient of dose can be seen in the results of the calculations using the MIRD-type phantom for the PA geometry, while the distribution of enamel doses is not clearly observed in the results of the calculations using the Voxel-type phantom and the ESR dosimetry for the same irradiation geometry. More photons are absorbed to soft tissue before reaching teeth in the MIRD-type phantom than the Voxel-type phantom and the physical phantom, as the mouth of MIRD-type is filled with soft tissue and the physical phantom has cavity area in the mouth.

Table 3 shows the comparison of the measured dose with TLDs and the results calculated by using the Voxel-type phantom. Numerical calculated enamel doses are also presented. The measured doses agree well with the results of the calculations, where the material of teeth region was defined as $CaSO_4$. The difference between the enamel dose and dose to teeth region with the material of $CaSO_4$ does not exceed 7% in the calculations using the same computational code and human model. It can be mentioned here that doses given by the measurements using TLDs indicate almost same values as the enamel doses against external exposure of 662keV and 1250 keV photons.

3.3 Comparison of calculated results between two human models

The calculated enamel doses by the two human models were compared in Table 4. The difference of the enamel dose between the two human models does not exceed 10% for energy region above 662keV, although there is an exception in the PA geometry of 662keV photons. The enamel dose by the Voxel-type phantom, however, is about 60% larger than that by the MIRD-type phantom in the case, where 30keV photons were incident to the body from the backside. This result suggests that the size and structure of the human head can affect the enamel dose against external exposure of low energy photons.

4. Conclusion

Enamel dose was quantitatively related to organ doses by the Monte Carlo calculations using EGS4 code and a modified MIRD-type phantom. The calculated enamel doses by using the Voxel-type phantom were valid to the results in the experiments. The model of the head did not significantly affect enamel doses for most cases. The enamel dose, however, can be influenced by the size and structure of the head for photons below 100keV. The conversion coefficients from enamel doses to organ doses obtained in this study [9] are to be useful for retrospective dose assessments by the ESR dosimetry using teeth.

References

1. Jacob, P., Bailiff, I., Bauchinger, M., Haskell, E. and Wieser, A., Retrospective Assessment of Exposures to Ionizing Radiation, ICRU NEWS June 2000, 5-11, (2000).

2. Ikeya, M., Miki, T., Kai, A. and Hoshi, M. ESR Dosimetry of A-Bomb Radiation Using Tooth Enamel and Granite Rock, Radiat. Dosim. Prot., 17, 181-184 (1986).

3. Serezhenkov, V.A., Dormacheva, E.V., Klevezal, G.A, Kulikov, S.M., Kuznetsov, S.A, Mordvintcev, P.I., Sukhovskaya, L.I., Schklovsky-Kordi, N.E., Vanin, A.F., Voevodskaya, N.V. and Vorobiev, A.I. Radiation Dosimetry for Residents of the Chernobyl Region: A Comparison of Cytogenetic and Electron Spin Resonance Method, Radiat. Prot. Dosim. , 42, 33-36, (1992).

4. Romanyukha, A.A., Ignatiev, E.A., Vasilenko, E.K., Drozhko, E.G., Wieser, A., Jacob, P., Keirim-Markus, I.B., Kleschenko, E.D., Nakamura, N. and Miyazawa, C. EPR Dose Reconstruction for Russian Nuclear Workers, Health Phys., 78(1), 15-20, (2000).

5. Iwasaki, M., Miyazawa, C., Uesawa, T., Suzuki, E., Hoshi, H. and Niwa, K. Exposure Rate Dependence of the CO33- Signal Intensity in ESR Dosimetry of Human Tooth Enamel, Radioisotopes, 41, 642-644 (1992).

6. Iwasaki, M., Miyazawa, C., Uesawa, T., Ito, I. and Niwa, K. Differences in Radiation Sensitivity of Human Tooth Enamel in an Individual and among the Individuals in Dental ESR Dosimetry, Radioisotopes, 44, 785-788 (1995).

7. Iwasaki, M., Miyazawa, C. and Uesawa, T. Effect of Tooth Position in the Oral Cavity for Various Irradiation Geometries in Dental ESR Dosimetry, Radioisotopes, 48, 530-534 (1999).

8. Cristy, M. Mathematical Phantom Representing Children of Various Ages for Use in Estimates of Internal Doses, MUREG/CR-1159 (1980).

9. Takahashi, F., Yamaguchi, Y., Iwasaki, M., Miyazawa, C. and Hamada, T., Relation between Tooth Enamel Dose and Organ Doses for the Electron Spin Resonance Dosimetry against External Photon Exposure, Radiat. Prot. Dosim. , 95, 101-108, (2001).

10. International Commission on Radiological Protection. Report of the Task Group on Reference man, ICRP Publication 23 (Oxford: Pergamon Press) (1974).

11. Nelson, W.R., Hirayama, H. and Rogers, D.W.O. The EGS4 Code System, SLAC-265 (1985).

12 . Takagi, S., Sato, O., Iwai, S., Uehara, T. and Nojiri, I. Development and Benchmarking of General Purpose User Code of EGS4, Proc. of the 1st International Workshop on EGS4 (Tsukuba), 86-96, (1997).

13. Trubey, D.K., Berger, M.J. and Hubbell, J.H. Photon Cross-Sections for ENDF/B-VI, Advanced in Nuclear Computation and Radiation Shielding, American Nuclear Society Topical Meeting (1989).

14. Zankl, M., Panzer, W. and Drexler, G., Topographic anthropomorphic models: Part II: organ doses from computed topographic examination in pediatric radiology, GSF-Berict No.30/93, Forschungszentrum fur Umwelt und Gesundheit, (1993).

15. Saito, K., Wittmann, A., Koga, S., Ida, Y., Kamei, T., Funabiki, J. and Zankl, M., The construction of a computed topographic phantom for a Japanese male adult and the dose calculation system, Radiat. Environ. Biophys, 40, 69 (2000).

16. Funabiki, J., Terabe, M., Zankl, M., Koga, S. and Saito, K., An EGS4 user code with Voxel geometry and a Voxel phantom generation system, Proc. of the 2nd International Workshop on EGS4, Tsukuba, Japan, 8-12 August, 2000, KEK Proceedings 2000-20, 56 (2000).

Table 1:
Absorbed dose to organ or tissue per air kerma in free air (Gy/Gy)

(A) 50 keV	AP	PA	RLAT	Angl. (Avr.)*
Red bone marrow	0.428	0.700	0.288	0.447
Lung	0.986	1.11	0.437	0.749
Stomach	1.34	0.464	0.0636	0.651
Bone Surface	1.95	2.40	1.38	1.86
Enamel	7.23	0.889	4.33	4.13
(B) 1250 keV	**AP**	**PA**	**RLAT**	**Angl. (Avr.)**
Red bone marrow	0.859	1.01	0.721	0.854
Lung	1.00	1.06	0.731	0.896
Stomach	1.09	0.815	0.450	0.832
Bone Surface	0.927	0.990	0.749	0.891
Enamel	1.04	0.624	0.956	0.889

** Values obtained by averaging doses all over horizontal incident angles*

Table 2:
Enamel dose distribution in a mouth for a 60Co source

(A) AP geometry	Relative value*		
	Front teeth	Middle teeth	Back teeth
ESR Dosimetry	1.0	1.0	0.9
Calculation (Voxel)	1.00	1.00	0.95
Calculation (MIRD)	1.00	0.95	0.90
(B) PA geometry	**Relative value***		
	Front teeth	**Middle teeth**	**Back teeth**
ESR Dosimetry	1.0	1.1	1.1
Calculation (Voxel)	1.00	0.95	1.06
Calculation (MIRD)	1.00	1.14	1.32

** The signal intensities or the enamel dose at middle and back part are relative values to those at front part, which are normalized to 1.0.*

Table 3:
Dose to teeth region per air kerma in free air (Gy/Gy)

Source, Geometry	Measurement	Calculation*1	
		$CaSO_4$*2	Enamel Dose
^{137}Cs, AP irradiation	1.04	1.01	1.05
^{60}Co, AP irradiation	0.929	0.949	0.976
^{60}Co, PA irradiation	0.672	0.646	0.689

**1: Human Model; Voxel-type phantom*
**2: Material of teeth region: $CaSO_4$ (TLD)*

Table 4:
Calculated enamel doses per air kerma in free air (Gy/Gy)

Photon energy (keV)	(a) AP geometry			(b) PA geometry		
	Voxel	MIRD	Voxel/MIRD	Voxel	MIRD	Voxel/MIRD
30 keV	1.90	1.94	0.979	0.0623	0.0375	1.66
50 keV	6.56	7.23	0.907	1.09	0.889	1.23
80 keV	5.97	6.97	0.857	1.77	1.60	1.11
150 keV	2.40	2.81	0.854	1.02	0.995	1.03
300 keV	1.28	1.45	0.883	0.662	0.604	1.10
662 keV	1.05	1.10	0.955	0.646	0.549	1.18
1250 keV	0.976	1.04	0.938	0.689	0.624	1.10
2500 keV	0.986	1.07	0.921	0.769	0.718	1.07

Figure 1:
Schematic view of (a) a MIRD-type phantom and (b) the cross section of head at the level of newly defined teeth-part.

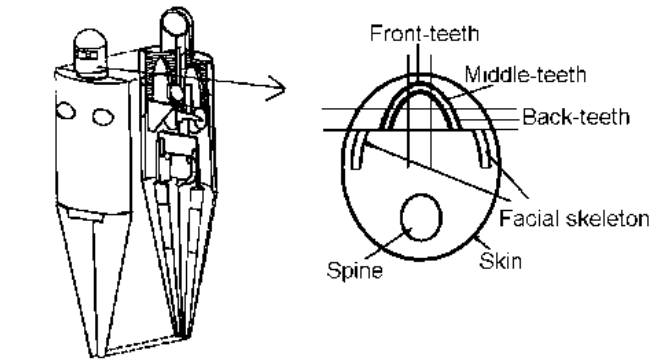

Figure 2:
Dose to organs or tissues per air kerma in free air as a function of photon energy for Angl. (Avr.) geometry.

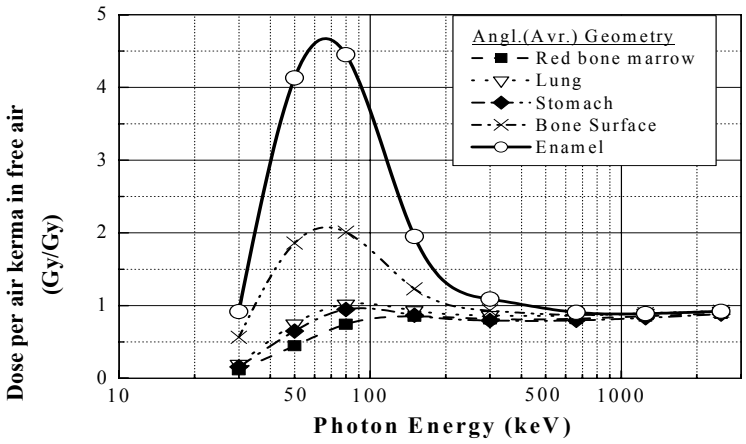

Figure 3:
Angular dependence of colon dose, thyroid dose and enamel dose for 1250keV photons.

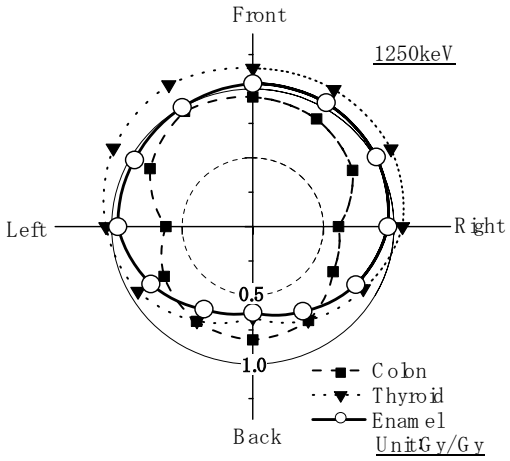

Dose Conversion Coefficients for High-Energy Radiations

Yukio Sakamoto, Shuichi Tsuda, Osamu Sato, Nobuaki Yoshizawa and Yasuhiro Yamaguchi

Yukio Sakamoto, Shuichi Tsud: Japan Atomic Energy Research Institute
Osamu Sato, Nobuaki Yoshizawa and Yasuhiro Yamaguchi: Mitsubishi Research Institute

Abstract

The dose conversion coefficients for high-energy radiations are indispensable for the shielding design of high-energy accelerator facilities and dose estimation against cosmic rays in high altitude flight. But there were no data of dose conversion coefficients for photons above 10 MeV and for neutrons above 180 MeV in the recent ICRP Publication 74. For photons, neutrons and protons up to 10 GeV and electrons up to 100 GeV, the absorbed dose to tissues and organs were calculated with Mote Carlo transport code system HERMES in conjunction with a MIRD-5 type anthropomorphic phantom, and the effective dose was evaluated by applying radiation weighting factors and tissue weighting factors. The effective dose equivalent was also evaluated by conventionally used quality factors.

At the same time, the Istituto Nazionale di Fisica Nucleare (INFN) group in Italy has been evaluating the effective dose and ambient dose equivalent with FLUKA code system. The effective dose conversion coefficients for photons and electrons above 10 MeV were almost same between two results. The effective dose for neutrons below 200 MeV was almost same between them, but there was maximum difference in the energy region from 1 GeV to 10 GeV by a factor of 2. The effective dose for protons in the energy range from 50 MeV to 10 GeV was also almost same between two results. From the comparison between effective dose and effective dose equivalent for neutrons and protons, it was proven that the radiation weighting factors proposed for high-energy neutrons and protons were overestimated from a viewpoint of effective quality factor.

New data of dose conversion coefficients for high-energy radiations are going to be more important for shielding design and dose evaluation in future construction of high-energy accelerator facilities.

Introduction

The dose conversion coefficients for high-energy radiations are needed in shielding designs of accelerator facilities and in dose estimation of cosmic rays in space missions and high altitude flight. In ICRP publication 51[(1)], there were dose conversion coefficients data for high-energy photons, electrons, positrons, neutrons, protons, pions and muons. In ICRP 1990 recommendations (ICRP publication 60[(2)]), a new concept of effective dose was introduced by using radiation-weighting factors, and the tissue weighting factors and Q-L relationship were changed. There were no data of dose conversion coefficients for high-energy radiations based on ICRP publication 60 at the early 1990s. So the evaluation of dose conversion coefficients was started for high-energy photons, electrons, neutrons and protons based on ICRP publication 60.

As protection doses for the human body, there are two kinds of dose, effective dose (E) and effective dose equivalent (H_E), defined by following formulas:

$$E = \Sigma w_T H_T = \Sigma w_T \Sigma w_R D_{T,R}$$
$$H_E = \Sigma w_T \hat{H}_T = \Sigma w_T \hat{Q}_T D_T$$

Where wR and DT,R are the radiation weighting factor and absorbed dose in tissue T for specific radiation, $\hat{Q}_T$ and DT are the averaged quality factor and absorbed dose in tissue T, wT is the tissue weighting factors for tissue T, HT and $\hat{H}_T$ are equivalent dose and dose equivalent of tissue.

The absorbed doses in each tissue and organ are calculated with a mathematical phantom model and radiation transport code. For the lower energy radiations, the difference between the effective dose and the effective dose equivalent is very small. The difference between the two doses has a great interest for high-energy radiations.

As the operational quantities for measurement, there is the ambient dose equivalent defined in ICRU sphere and slab phantom. The difference between the effective dose and the ambient dose equivalent also has a great interest for high-energy radiations.

Status Of Dose Conversion Coefficients

The status of dose conversion coefficients for high-energy radiations is shown in Table 1. In ICRP publication 51, the ambient dose equivalents in the slab phantom with 30 cm thickness, 1 cm depth dose equivalent and maximum dose equivalent, were cited. The upper energies were 20 GeV for photons and electrons, and 100 GeV for neutrons and protons. These data were based on old Q-L relations. In ICRP publication 74[3], the effective doses based on ICRP publication 60 were cited, but these data were limited below 10 MeV for photons and electrons, and 180 MeV for neutrons. There were no data for protons.

In Japan, the effective doses were evaluated for photons[4], neutrons and protons[5,6] up to 10 GeV and for electrons[7] up to 100 GeV with HERMES code system[8]. The effective dose equivalents[5,6] were also evaluated by using same tissue weighting factors. INFN, Italian group has evaluated the effective doses[9] for photons and electrons up to 100 GeV, and for neutrons and protons up to 10 TeV with FLUKA code system[10]. They evaluated also the ambient dose equivalents[9]. IHEP group of Russia evaluated the ambient dose equivalents[11] for neutrons with HADRON code[12]. Recently, Georgia Tech. Group of USA evaluated the effective dose[13] for photons and neutrons with MCNPX code[14].

Calculation Method

The component of HERMES code system established by KFA is shown in Figure 1. The hadrons cascade code, HETC-kFA2 simulates the behaviors of neutrons, protons, ions with mass heavier than 10, pions, muons and residual nuclides. The behaviors of neutrons below 15 MeV and secondary photons are simulated with MORSE-CG code. NDEM code calculates the photon spectra from de-excitation of excited residual nuclei. The behaviors of electrons, positrons and photons are simulated with electro-magnetic cascade code EGS4[15]. For the evaluation of dose equivalents, the quality factor database of secondary charged particles was developed for a wide energy range and kerma factors weighted with

quality factors were developed for neutrons below 15 MeV. As the mathematical phantom model, the MIRD-5 type phantom[16] was used.

Averaged quality factors for pions, protons, α and ^{16}O charged particles based on new Q-L relationship[2] up to 100 GeV are shown in Figure 2. Averaged quality factors were obtained by the averaging of quality factors from incident energy to stoppage energy. The curves for pions and protons have single peak, and the curves of heavy ions have two peaks. The Q-L relationship and stopping powers of charged particles against energies are shown in Figure 3. The maximum stopping power of pions and protons is smaller than 100 keV per micrometer. So these particles give only one peak. In the case of heavy ions with maximum stopping power over 100 keV per micrometer, one peak corresponds to the maximum value of Q-L relationship and the other peak corresponds to the maximum of linear energy transfer.

The quality factors are defined by the final charged particles, which deposit the energy into the human tissues and organs. On the other hand, the radiation weighting factors are defined by the incident radiation, itself.

Dose Conversion Coefficients For Photons

In Figure 4, the effective dose per unit photon fluency at Anterior-Posterior irradiation, front irradiation is shown. The filled circles and triangles give the HERMES code results[4] and FLUKA code results[9], respectively. Two results gave almost same behaviors. These results included the effect of electron transport. As the electrons produced by the high-energy photons in the human body penetrated tissues and organs, effective dose approached the constant above 1 GeV. In Figure 4, open circles give the results with kerma approximation, that was no electron transport and the energy of electrons and positrons was deposited in the vicinity of collided point. It was proved that the results with kerma approximation overestimated the results including the electron transport above 50 MeV. In the low energy, AP irradiation gave the maximum dose among irradiations. As the energy increase, the maximum dose was shifted to Posterior-Anterior and Lateral geometries.

Figure 5 shows the ambient dose equivalent per unit photon fluency at each depth of ICRU sphere with maximum effective dose. Square symbols give the maximum effective doses among irradiation geometries. It was proved that the 1 cm depth dose equivalent was not the proper operational quantity for high-energy photons, and the 15 cm or 20 cm depth dose equivalents were very similar to the maximum effective dose.

Dose Conversion Coefficients For Electrons

Figure 6 shows the effective dose per unit electron fluency at AP irradiation. Filled circles and triangles give the results calculated with HERMES code[7] and FLUKA code[9], respectively. Two results gave almost same behaviors and effective dose approached the constant above 50 MeV. As the electrons and positrons in the human body occurred the energy deposition, the effective dose per unit electron fluency was greater than that per unit photon fluency from the viewpoint of efficiency of electron production.

For the very high-energy electrons, the contribution of hadrons cascades to dose was large with the contribution of electromagnetic cascades. Hadrons such as neutrons and protons were produced by the photonuclear reaction, for example, (γ, n) reaction. The degree of secondary particle contribution to absorbed dose was estimated to be about 1 % and that contribution to dose equivalent was estimated to be about 5 %.

Dose Conversion Coefficients For Neutrons

Figure 7 shows effective doses and effective dose equivalents per unit neutron fluency at AP irradiation. Filled circles and triangles give effective doses of HERMES code's results[5,6] and FLUKA code's results[9], respectively. The two results gave almost same behaviors below 500 MeV, but there was some difference between the two results above 1 GeV. This was caused by the difference of cross section data. Open circles give the effective dose equivalents per unit neutron fluency at AP irradiation. There was large difference between effective dose and effective dose equivalent. As the absorbed doses and tissue weighting factors of each tissue were same ones, the difference was caused by the difference between radiation weighting factors and averaged quality factors.

Quality factors averaged over body[5,6] and radiation weighting factors[2] for neutrons are shown in Figure 8. Symbols of filled circles, open circles and boxes give quality factors averaged over body for AP, PA and ISO irradiations. Lines including the broken lines give radiation-weighting factors cited in ICRP publication 60. From the comparison between quality factors averaged over body and radiation weighting factors, the latter was about 30 % overestimated for neutrons above 100 MeV.

Dose Conversion Coefficients For Protons

Figure 9 shows effective doses and effective dose equivalents per unit proton fluency at AP irradiation. Filled circles and triangles give effective doses of HERMES code's results[5,6] and FLUKA code's results[9], respectively. HERMES code's results were greater than FLUKA code's results below 50 MeV and from 1 GeV to 2 GeV regions. This was caused by the difference of cross section data as same as neutron case. Open circles give the effective dose equivalents of HERMES code's results[5,6]. There was also large difference between effective dose and effective dose equivalent.

Quality factors averaged over body and radiation-weighting factors[2] for protons are shown in Figure 10. Symbols of filled circles, open circles and boxes give quality factors averaged over body[5,6] for AP, PA and ISO irradiations obtained with HERMES code[5,6]. Line gives the radiation-weighting factor (w_{ry}=5) cited in ICRP publication 60. Two types of triangles give averaged quality factors at 1cm depth and maximum dose positions of ICRU sphere with FLUKA code[9].

Averaged quality factors gave almost same behaviors between HERMES code and FLUKA code calculations. The radiation weighting factors were larger than quality factors averaged over body by a factor of 2.5 above 100 MeV protons.

Summary

A new data set of dose conversion coefficients based on ICRP 1990 recommendations for high-energy photons, electrons, neutrons and protons was evaluated by using HERMES code system and the MIRD-5 type phantom. HERMES code's results were almost same results calculated with FLUKA code systems but there were some differences in neutron and proton doses caused by the differences of cross section data. From the comparison between effective doses and effective dose equivalents for neutrons and protons, it was proved that radiation weighting factors for neutrons and protons cited in ICRP publication 60 were larger than quality factors averaged over body.

In the OECD/NEA SATIF group, accelerator shielding task group, cross section data and absorbed dose has been compared[17].

References

1. International Commission on Radiological Protection, "Data for Use in Protection Against External Radiations: ICRP Publication 51", Ann. ICRP 17, No.2/3 (1987).
2. International Commission on Radiological Protection, "1990 Recommendations of the International Commission on Radiological Protection: ICRP Publication 60", Ann. ICRP 21 (1-3) (Oxford: Pergamon) (1991).
3. International Commission on Radiological Protection, "Conversion Coefficients for Use in Radiological Protection Against External Radiation: ICRP Publication 74", Ann. ICRP 26 (3/4) (Oxford: Elsevier Science) (1996).
4. Sato, O., Yoshizawa, N., Takagi, S., Iwai, S., Uehara, T., Sakamoto, Y., Yamaguchi, Y. and Tanaka, S., "Calculations of Effective Dose and Ambient Dose Equivalent Conversion Coefficients for High Energy Photons", J. Nucl. Sci. Technol., 36, 977 (1999).
5. Yoshizawa, N., Sato, O., Takagi, S., Furihata, S., Iwai, S., Uehara, T., Tanaka, S. and Sakamoto, Y., "External Radiation Conversion Coefficients using Radiation Weighting Factor and Quality Factor for Neutron and Proton from 20 MeV to 10 GeV", J. Nucl. Sci. Technol., 35, 928 (1998).
6. Yoshizawa, N., Sato, O., Takagi, S., Furihata, S., Funabiki, J., Iwai, S., Uehara, T., Tanaka, S. and Sakamoto, Y., "Fluence to Dose Conversion Coefficients for High-Energy Neutron, Proton and Alpha Particles", J. Nucl. Sci. Technol., Supplement 1, 865 (2000).
7. Tsuda, S., Endo, A., Yamaguchi, Y. and Sato, O., "Fluency to Effective Dose Conversion Coefficients for Electrons from 1 MeV to 100 GeV", Radiat. Prot. Dosim. 95, 5 (2001).
8. Cloth, P., Filges, D., Neef, E.D., Sterzenbach, G., Reul, Ch., Armstrong, T.W., Colborn, B.L., Anders, B. and Brückmann, H., "HERMES: A Monte Carlo Program System for Beam-Materials Interaction Studies", Jül-2203 (1988).
9. Pelliccioni, M., "Overview of Fluence-to-Effective Dose and Fluence-to-Ambient Dose Equivalent Conversion Coefficients for High Energy Radiation Calculated Using the FLUKA Code", Radiat. Prot. Dosim. 88, 279 (2000).
10. Fassò, A., Ferrari, A., Ranft, J. and Sala, P.R., "*New Developments in FLUKA Modeling of Hadronic and EM Interactions",* in Proc. of the Third Workshop on Simulating Accelerator Radiation Environments (SARE-3), Tsukuba (Japan), Hirayama, H. ed., KEK Proceedings 97-5, 32 (1997).
11. Sannikov, A.V. and Savitskaya, E.N., "*Ambient Dose Equivalent Conversion Factors for High Energy Neutrons on the ICRP-60 Recommendations",* Radiat. Prot. Dosim. 70, 383 (1997).
12. Savitskaya, E.N. and Sannikov, A.V., "*High Energy Neutron and Proton Kerma Factors for Different Elements",* Radiat. Prot. Dosim. 60, 135 (1995).
13. Sutton, M.R., Hertel, N.E. and Wtears, L.S, "*Fluence-to-Effective Dose Conversion Coefficients for High-Energy Radiations Calculated with MCNPX",* in Proc. of the Fifth Meeting of the Task Force on Shielding Aspects of Accelerators, Tragets and Irradiation Facilities (SATIF-5), Paris (France), July 2000, OECD/NEA Nuclear Science Documents, 297 (2001).
14. Hughes, H.G., Prael, R.E. and Little, R.C., "*MCNPX – The LAHET/MCNP Code Merger",* Los Alamos National Laboratory, XTM-RN(u) 92-012 (1997).
15. Nelson, W. R., Hirayama, H. and Rogers, D. W. O., "*The EGS4 Code System",* SLAC-265 (1985).
16. Yamaguchi, Y., "*DEEP Code to Calculate Dose Equivalents in Human Phantom for External Photon Exposure by Monte Carlo*", JAERI-M 90-235 (1990).
17. Yoshizawa, N., Sakamoto, Y., Iwai, S. and Hirayama, H., "*Benchmark Calculation with Simple Phantom for Neutron Dosimetry",* in Proc. of the Fifth Meeting of the Task Force on Shielding Aspects of Accelerators, Targets and Irradiation Facilities (SATIF-5), Paris (France), July 2000, OECD/NEA Nuclear Science Documents, 253 (2001).

Table 1:
Status of dose conversion coefficients for high-energy radiations.

RADIATION	ICRP 51[1] $H^*(10), H_{MAX}$	ICRP 74[3] E	JAERI/MRI[4,5,6,7] E	INFN[9] E
PHOTONS	≤20GeV	≤0.01GeV	≤10GeV	≤100GeV
ELECTRONS			≤100GeV	
NEUTRONS	≤100GeV	≤0.18GeV	≤10GeV	≤10,000GeV
PROTONS		-		
	slab phantom	$H^*(10)$	H_E (HERMES code)	$H^*(10), H_{max}$ (FLUKA code)

Others: IHEP(HADRON code, n, $H^*(10)$)[11], Georgia Tech. (MCNPX code, γ, n, E)[13]

Figure 1:
Organization of HERMES Code System and Phantom Model.

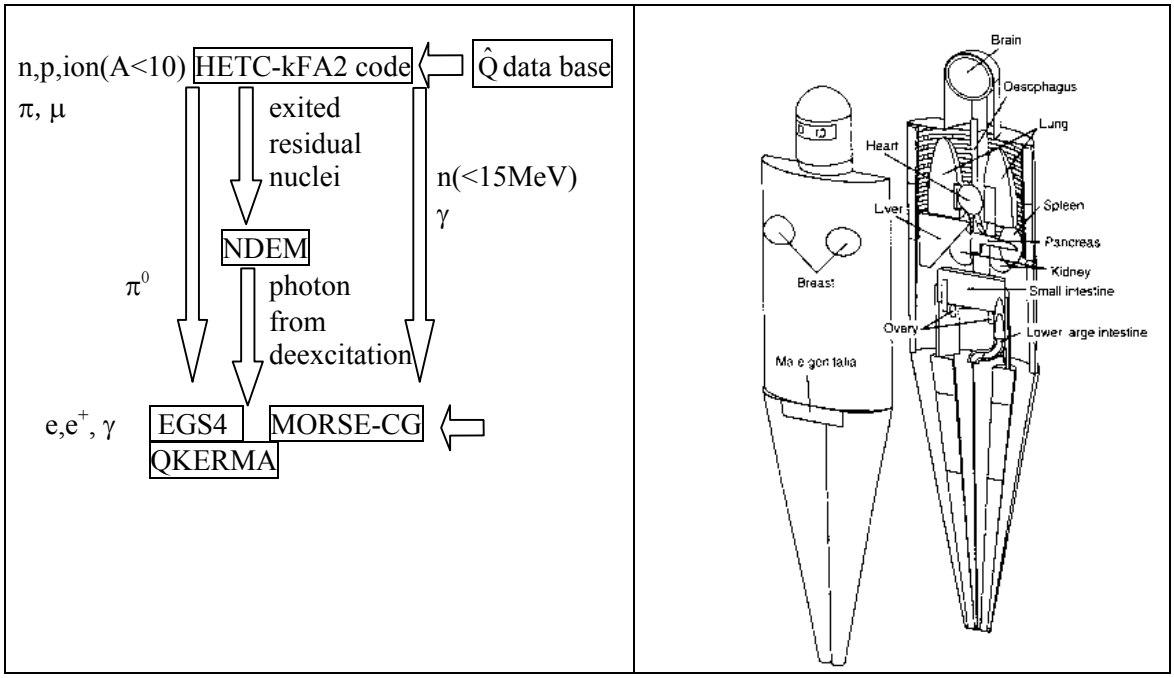

Figure 2:
Averaged quality factor of charged particle.

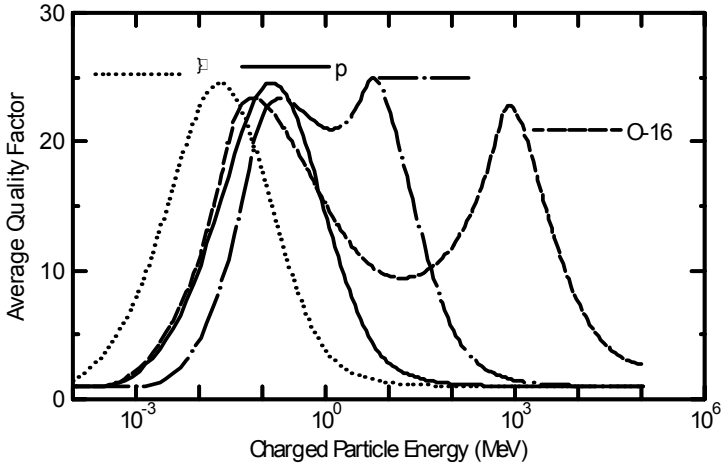

Figure 3:
LET of charged particles and Q-L relation.

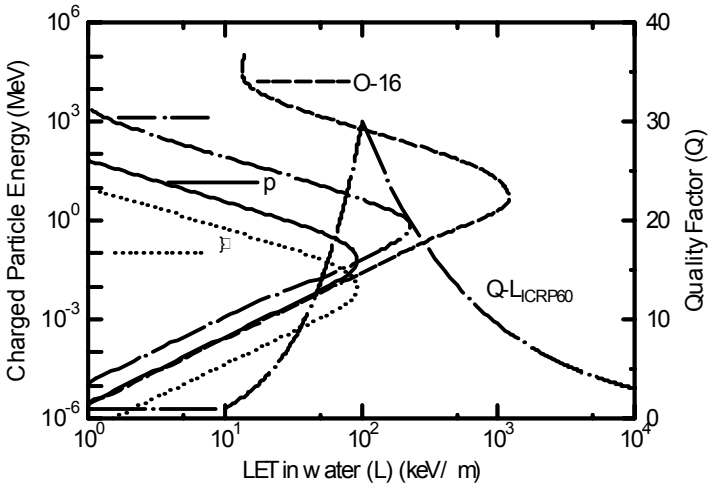

Figure 4:
Effective dose for photons

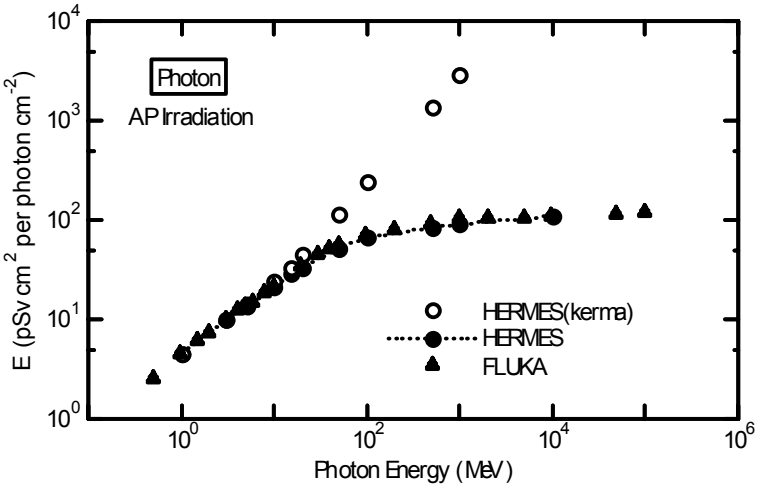

Figure 5:
Ambient dose equivalent for photons

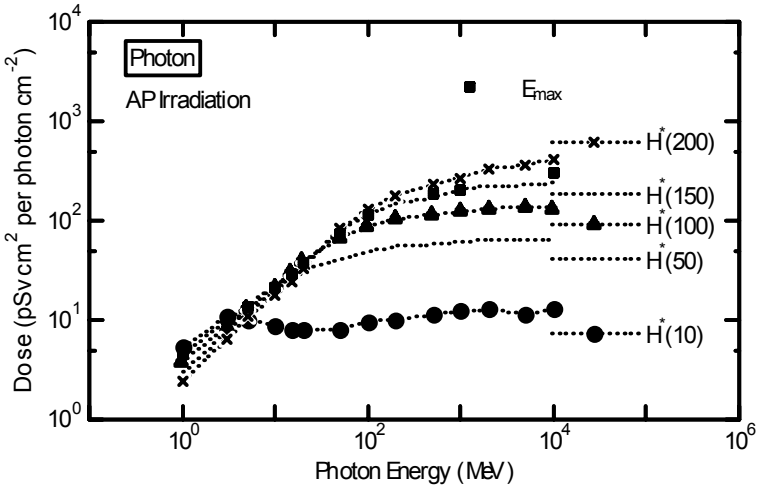

Figure 6:
Effective dose for electrons

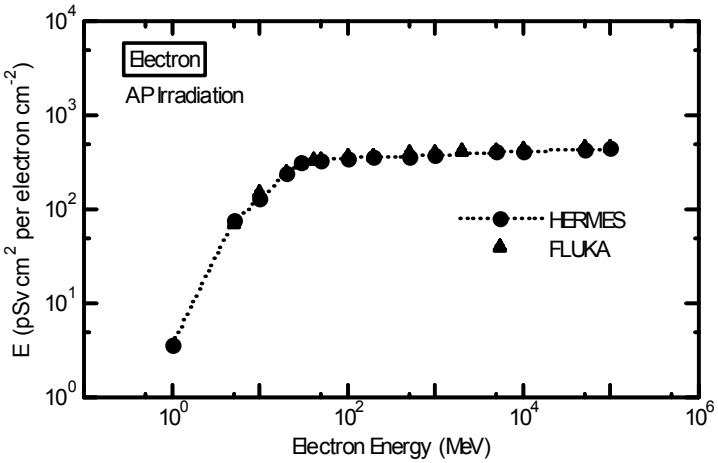

Figure 7:
Doses for neutrons

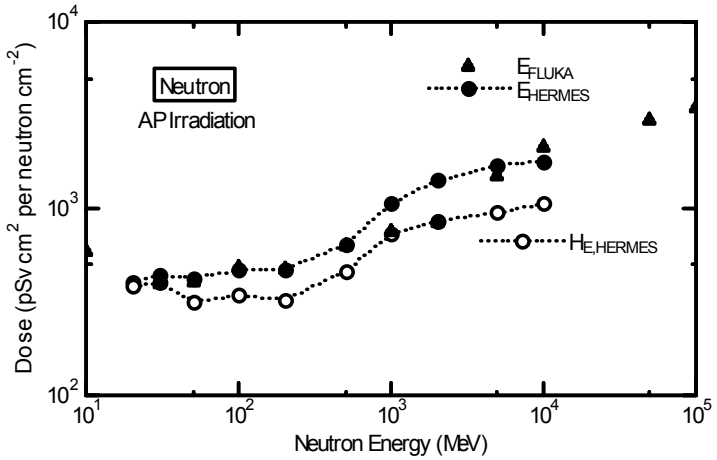

Continue